This manuscript is a non reviewed preprint. The manuscript has not yet been submitted for publication. This is third uploaded and improved version. Subsequent versions of this manuscript will have updated content, including the journal of submission and DOI.

Feedback is encouraged, questions are welcomed, feel free to contact the author:

stanislav.jelavic@sund.ku.dk

Fate of organic compounds during transformation of ferrihydrite in Precambrian iron formations

S. Jelavić,[1,2*] A. C. Mitchell[3] and K.K. Sand[1,2,3]

[1]Nano-Science Center, Department of Chemistry, University of Copenhagen, Universitetsparken 5, Copenhagen, Denmark

[2]Section for GeoGenetics, Globe Institute, University of Copenhagen, Øster Voldgade 5-7, Copenhagen, Denmark

[3]Aberystwyth University, Department of Geography & Earth Sciences, Aberystwyth, UK

[*]stanislav.jelavic@sund.ku.dk

ABSTRACT

The absence of organic compounds from Precambrian iron formations (IF) challenges the hypothesis of their biogenic origin. Here we address the fate of adsorbed organic compounds during transformation from ferrihydrite to hematite. We determined the binding energy between hematite and common molecular terminations found in extracellular polymeric substances and biofilms: carboxylic, alcohol and phosphate functional groups. We found that the bond between hematite and alcohol group is approximately 2 times stronger than the bond between hematite-carboxyl and -phosphate groups. We transformed synthetic ferrihydrite to hematite in presence of glycerol, which has a high density of alcohol groups and measured the amount of mineral associated glycerol before and after the transformation. We show that the transformation releases glycerol highlighting that organic compounds adsorbed at precursor ferrihydrite could be desorbed already during the process of IF sedimentation and diagenesis. Our results suggest that the absence of organic compounds in IF should not be used as evidence against their biogenic origin.

Introduction

Traditionally, iron formations (IFs) have been considered as abiotically generated chemical sediments but an increasing body of evidence suggests the active role of microbes in their precipitation (Koehler *et al.*, 2010). The role of anoxygenic phototrophic bacteria in the formation of IFs has been speculated since the work of Garrels *et al.* (1973). An improved understanding of microbially induced Fe oxidation highlights that oxidizing bacteria, such as *Rhodobacter ferrooxidans*, could likely drive the formation of IFs (Kappler *et al.*, 2005). Further, mass balance calculations have showed that Fe (II)-oxidising phototrophic bacteria have the capacity to oxidise all Fe(II) from the Precambrian ocean, causing formation of iron (oxyhydr)oxide (FeOx) (Hegler *et al.*, 2008). However, the low concentration of organic compounds in IFs and their diagenetic or metamorphic derivatives, challenges the hypothesis of their biogenic origin (Klein, 2005).

Extracellular polymeric substances (EPS) promote FeOx nucleation (Sand *et al.*, 2019) where microbially formed FeOx are often found in close association with the EPS (Chan *et al.*, 2004). When EPS is encrusted with FeOx, the polymers are shed and new EPS are formed. This prevents the encrustation of the microbe itself (Phoenix *et al.*, 2000; Chan *et al.*, 2004). During IF formation, FeOx-EPS composites would have settled through the water column and be deposited on the sea floor. Such a mechanism of IF deposition implies the presence of a significant concentration of organic compounds in freshly deposited FeOx. However, there is evidence that the depositional environment was most likely scarce in organic compounds (Dodd *et al.*, 2019) thus themajority of the organic compounds must have been lost prior to deposition.

Hematite is a major component of IFs found today (Konhauser *et al.*, 2017) but, initially, the FeOx in the FeOx-polymer complexes were most likely composed of ferrihydrite (Chan *et al.*, 2004). The transformation to hematite would have happened both before (Sun *et al.*, 2015) and after deposition on the seabed. Depending on the solution conditions, ferrihydrite to hematite transformation can involve lepidocrocite and goethite as intermediary phases, *e.g.*, through Fe(II) catalysed transformation (Hansel *et al.*, 2003), or it can be direct (Cudennec & Lecerf, 2006). Transformation involving intermediary phases is a dissolution-precipitation process (Schwertmann & Murad, 1983) implying that the interface between ferrihydrite and organic compounds is eliminated. In this scenario, organic compounds would have been liberated to

solution where they could have been readsorbed to the newly formed phases or released in the water column and subsequently degraded. The direct transformation from ferrihydrite to hematite is a solid-state transition where atoms move only locally to occupy new structural positions (Cudennec & Lecerf, 2006), without the loss of interface with adsorbed complexes. Thus, the direct transformation of ferrihydrite to hematite is not necessarily accompanied by a removal of organic compounds. However, the Gibbs free energy of binding (ΔG_{bu}) between ferrihydrite and EPS is larger than between hematite and EPS (Sand *et al.*, 2019) implying that the polymers were more likely to desorb from hematite than from ferrihydrite. In such a case, the absence of organic compounds in IFs cannot be an argument against their biogenic origin.

To better understand the fate of adsorbed organic compounds during direct transformation from ferrihydrite to hematite, we used dynamic force spectroscopy (DFS) to measure the energy of binding between hematite and organic functional groups represented in EPS. Subsequently we identified the functional group least likely to desorb during transformation and made transformation experiments where we used thermogravimetric analysis (TGA) to measure the loss of organic compounds during transformation.

Materials and Methods

DFS. We used an Asylum MFP3D atomic force microscope (AFM) and functionalized gold coated AFM tips (MSCT, Bruker) with carboxyl (COO^-), alcohol (OH), and phosphate (HPO_4^-) headgroups pointing away from the AFM probe (Fig. 1a). Tips were functionalized following the protocol described in Jelavić *et al.* (2017) (details in SI).

Specular hematite monocrystal {0001} face was cleaned prior to analysis following the protocol described in Jelavić *et al.* (2017) (details in SI). For DFS measurements, we collected >500 force curves per experiment. The tip approaching velocity was set to 500 nms^{-1} and the retraction velocity varied between 10 - 10000 nms^{-1}. The trigger force was set to 100 pN and dwell time to 0.5 s. During the measurement, the head groups bound to the hematite surface (Fig. 1a) and we measured the forces applied to break the bond (i.e. the force curve, Fig. 1b). We fit the rupture forces vs. the loading rate to a multibond model (Friddle *et al.*, 2012) enabling calculation of ΔG_{bu} (Eq. S1-S4). The measurements were done in 10 mM NaCl solution at pH=5.6. We chose this conditions, rather than conditions at which the transformation experiments were conducted, to maximise the interaction forces between the tip and hematite surface (Lützenkirchen *et al.*, 2013; Newcomb *et al.*, 2017).

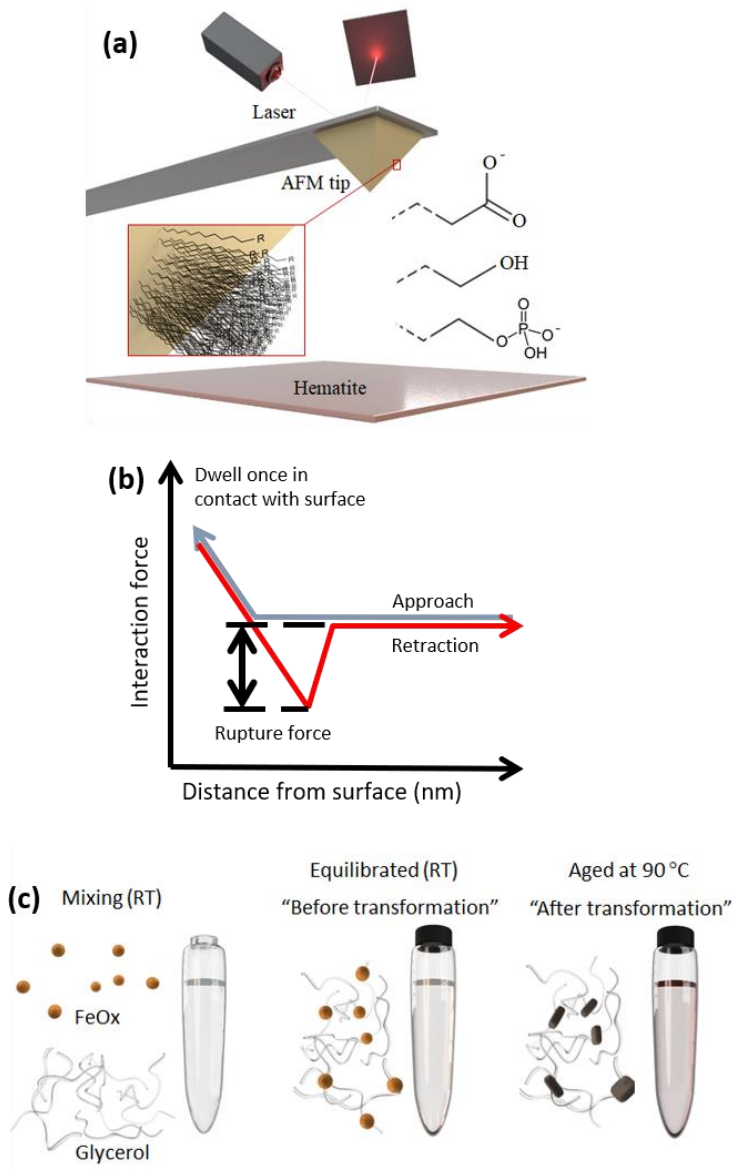

Figure 1. a) Schematics of the DFS: SAMs with carboxyl, alcohol and phosphate headgroups covalently bonded to AFM tip. **b)** A scheme of a force curve. **c)** In transformation experiments, ferrihydrite and glycerol were mixed at room temperature and left to equilibrate overnight. One sample was then taken for TGA (equilibrated sample) and the rest was placed in the oven at 90 ºC until the transformation was complete (aged sample).

Transformation experiments. Ferrihydrite was synthesised using the method of Schwertmann & Cornell (2000). We used 0.5 M NaCl solution and pH=7 as a proxy for Precambrian seawater. We chose glycerol (CH_2**OH**-CH**OH**-CH_2**OH**) as a model for an OH-rich molecule. Adsorption of polymers is a complex function of degree of branching, length and hydrophobicity (van Oss, 1997).

The aim here is not to account for such variations but to isolate the effect of ΔG_{bu} on the magnitude of desorption during transformation. We mixed 15 mg of ferrihydrite with 15 ml of 0.5 M NaCl and added glycerol to a final concentration of 0.5% (Fig. 1c). In control samples, we omitted glycerol. Samples were shaken at 100 rpm overnight to equilibrate. The next day, a batch of samples was rinsed with 20 ml of 0.5 M NaCl (adjusted to pH=7 with 1 M NaOH) by ultracentrifugation (equilibrated sample). Another batch was placed in the oven heated to 90 °C, and once the transformation was over, the samples were rinsed with 20 ml of 0.5 M NaCl and adjusted to pH=7 (aged sample). The samples from the oven were sampled at specific time steps to follow the transformation pathway using X-ray diffraction (XRD). All samples were freeze dried after rinsing.

XRD. Samples for XRD were washed with ultradeionised water. 1.5 ml of suspension was pipetted on the zero background Si holders and left to dry at room temperature. We collected diffractograms in reflection mode on the Bruker D8 Advance instrument using Cu Kα radiation (λ = 1.5418 Å) operated at 40 kV and 40 mA, and a LynxEye detector. Diffractograms were collected from 10-90 °2θ with step size of 0.02° and 1.7 s counting time per step. The sample was spun at 20 rpm. We used 0.3° divergence and 3° antiscatter slits, 2.5° Soller slits on incident and diffracted beams and a 0.02 mm thick Ni-filter. The opening of detector window was 2.94°.

TGA. We used Netzsch TG 209 F1 Libra. Samples were heated at a rate of 10 °Cmin^{-1} from 30 to 1000 °C under N_2 atmosphere. ~15 mg of sample was placed into the Pt crucible and the weight loss was measured as a function of temperature.

TEM. Images were taken with a Philips CM 20 TEM equipped with a thermionic LaB_6 filament. We used an accelerating voltage of 200 kV. Samples were prepared by placing a droplet of sample suspension on a formvar coated TEM grid and left for 5 - 10 s. Subsequently, the grid was washed in ultradeionised water and water droplets were removed with the edge of a paper towel.

Results and Discussion

Energy of binding. The force spectra (Fig. 2) shows that the rupture force between hematite and the OH group is ~6 times higher than between COO^- and HPO_4^- groups (Fig. 2, Table S-1). Recalculated to ΔG_{bu} (Eq. S-4), that is an increase in ~2 kT. Considering that the {0001} hematite surface is completely hydroxylated in water (Trainor *et al.*, 2004), our results follow the trend where OH-OH bonds are twice as strong as COO^--OH bonds at circumneutral pH (Vezenov *et al.*, 1997) present in Precambrian ocean. Thus, irrespective of the transformation pathway, biopolymers rich in acidic groups desorb more easily from hematite than those rich in alcohol groups.

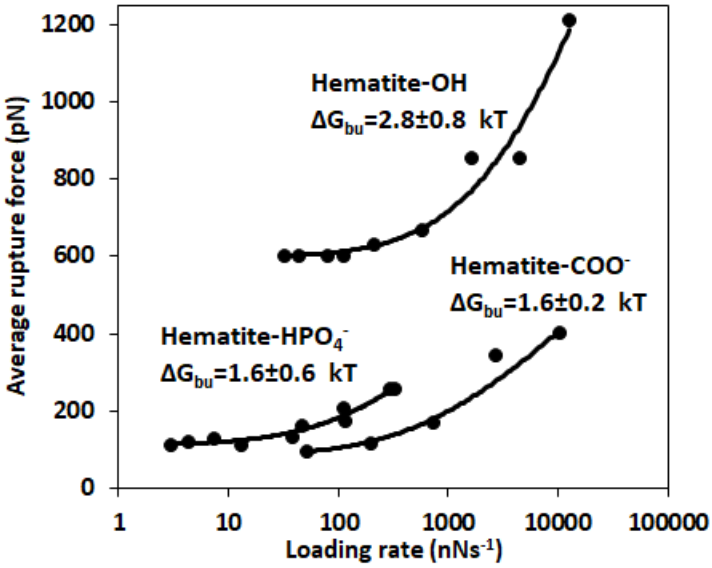

Figure 2. Multibond fit (Friddle *et al.*, 2012) to the dynamic force spectra between hematite surface and alkyl thiol SAMs with OH, HPO_4^- and COO^- head groups. The uncertainty represents the error propagated from the standard deviations of the fit. Loading rate is a nominal retraction velocity (nms^{-1}) multiplied with the spring constant of the cantilever ($nNnm^{-1}$).

Transformation pathway. To investigate the fate of a ferrihydrite-associated OH-containing molecule during transformation to hematite, we transformed the ferrihydrite-glycerol complex, monitored the transformation pathway with XRD and determined the weight loss with TGA. The ferrihydrite-glycerol complex transformed directly to hematite without any intermediary phases (Fig. S-2) suggesting a solid-state transformation pathway. As a control, we transformed ferrihydrite in absence of glycerol using the same solution conditions. Even though the hematite

was the first phase to occur after 17 h, goethite started forming after 43 h (Fig. S-1) indicating that, in pure system, some ferrihydrite dissolves and reprecipitates as goethite, as previously shown (Das *et al.*, 2011).

The transformation is accompanied by glycerol release. In general, the ferrihydrite-gycerol complex lost more weight than the pure ferrihydrite (Fig. 3, Table 1). Ferrihydrite is more hydrated than hematite so the loss of loosely adsorbed water (<125 ºC) and tightly bound water (125-700 ºC) is higher for ferrihydrite than hematite (Hiemstra & Van Riemsdijk, 2009). Comparing the weight loss of ferrihydrite-glycerol (5.4%, Table 1) to pure ferrihydrite (4.7%) in the 125-700 ºC range, shows that the tightly bound water accounts only for 87% of the weight loss in this region, indicating that the remaining 13 % is the loss of glycerol. This implies that hematite produced by aging ferrihydrite-glycerol contains less glycerol than the original ferrihydrite-glycerol (equilibrated), and that glycerol is released during transformation.

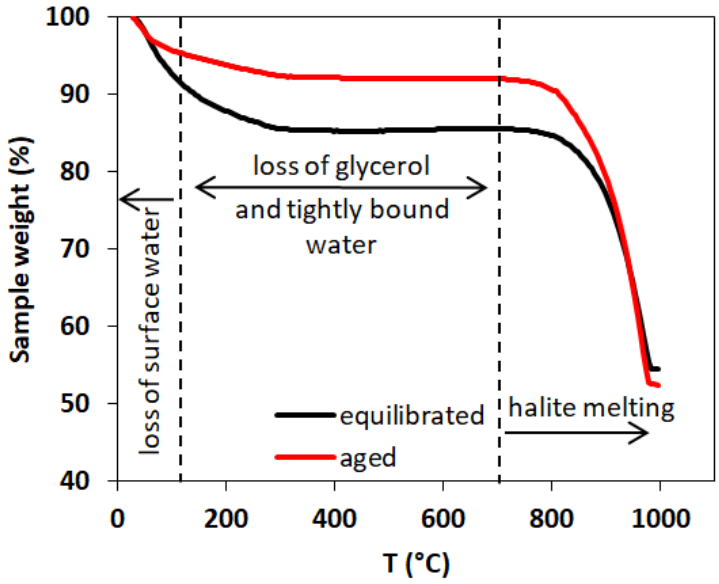

Figure 3. Comparison of TG curves of ferrihydrite-glycerol (equilibrium-black curve) and resulting hematite-glycerol (aged- red curve). The smaller mass loss in the region 125-700 °C (dashed vertical lines) for the aged sample compared to the equilibrium sample suggests bigger loss of tightly bound water and glycerol during the transformation.

Table 1. Weight loss during the TGA analysis in <125 °C and 125-700 °C regions.

Sample		% weight loss	
		<125 °C	125-700 °C
Glycerol	equilibrated	8.9	5.4
	aged	4.8	3.2
Control	equilibrated	9.8	4.7
	aged	n.a.*	n.a.

* transformation yielded both goethite and hematite making comparison impossible

The reason for the loss of the glycerol during transformation can also be the smaller specific surface area (SSA) of the produced hematite (Fig. S-3) and not only the lower affinity for glycerol compared to ferrihydrite. From TEM images, we estimated the SSA of ferrihydrite to be 374-790 m^2g^{-1} and of hematite to be 10-46 m^2g^{-1}. Thus, the decrease in the SSA during transformation is between 9-70 times which alone is possible to explain the decrease in glycerol content. However, the loss must be amplified by the lower ΔG_{bu} for hematite-OH than for ferrihydrite-OH system. Both the decrease of SSA and the decrease of ΔG_{bu} are likely explanations for our observations and both scenarios are likely to have contributed to the loss of organic compounds during the formation of IFs.

We have demonstrated that glycerol, a molecule with a high ΔG_{bu} to hematite, desorbs during the transformation of ferrihydrite to hematite. We propose that a significant mass of organic compounds from FeOx-EPS composites is desorbed early in the process of FeOx sedimentation because of the transformation from ferrihydrite to hematite. This loss of organic compounds is probably further enhanced by the grain coarsening of hematite during diagenetic and metamorphic processes. Our experiments were designed to determine the loss of strongly bound molecules from FeOx during the direct transformation, which is least likely to result in desorption of adsorbed organic compounds. The less-strongly bound organic compounds or organic compounds adsorbed to ferrihydrite that transformed via dissolution-precipitation pathway would likely have desorbed in higher proportion than what we report here. Thus, our results highlight that the absence of organic compounds in IF should not be used as evidence against their biogenic origin.

ACKNOWLEDGMENTS

We thank Heloisa N. Bordallo for access to TGA instrument (Carlsbergfondets, grant no. 2013_01_0589). KKS and ACM are grateful for funding from the European Union's Horizon 2020 Research and Innovation Programme under Marie Skłodowska-Curie Grant Agreement No 663830 and the Welsh Government and Higher Education Funding Council for Wales through the Sêr Cymru National Research Network for Low Carbon, Energy and Environment. KKS is grateful for funding from the Danish Council for Independent Research Sapere Aude Programs (0602-02654B).

REFERENCES:

Chan, C.S., Stasio, G.D., Welch, S.A., Girasole, M., Frazer, B.H., Nesterova, M.V., Fakra, S., Banfield, J.F. (2004) Microbial Polysaccharides Template Assembly of Nanocrystal Fibers. *Science* 303, 1656–1658.

Cudennec, Y., Lecerf, A. (2006) The transformation of ferrihydrite into goethite or hematite, revisited. *Journal of Solid State Chemistry* 179, 716–722.

Das, S., Hendry, M.J., Essilfie-Dughan, J. (2011) Transformation of Two-Line Ferrihydrite to Goethite and Hematite as a Function of pH and Temperature. *Environmental Science & Technology* 45, 268–275.

Dodd, M.S., Papineau, D., Pirajno, F., Wan, Y., Karhu, J.A. (2019) Minimal biomass deposition in banded iron formations inferred from organic matter and clay relationships. *Nature Communications* 10, 1–13.

Friddle, R.W., Noy, A., Yoreo, J.J.D. (2012) Interpreting the widespread nonlinear force spectra of intermolecular bonds. *Proceedings of the National Academy of Sciences* 109, 13573–13578.

Garrels, R.M., Perry, E.A., Mackenzie, F.T. (1973) Genesis of Precambrian Iron-Formations and the Development of Atmospheric Oxygen. *Economic Geology* 68, 1173–1179.

Hansel, C.M., Benner, S.G., Neiss, J., Dohnalkova, A., Kukkadapu, R.K., Fendorf, S. (2003) Secondary mineralization pathways induced by dissimilatory iron reduction of ferrihydrite under advective flow. *Geochimica et Cosmochimica Acta* 67, 2977–2992.

Hegler, F,, Posth, N.R., Jiang, J., Kappler, A. (2008) Physiology of phototrophic iron(II)-oxidizing bacteria: implications for modern and ancient environments. *FEMS Microbiology Ecology* 66, 250–260.

Hiemstra, T., Van Riemsdijk, W.H. (2009) A surface structural model for ferrihydrite I: Sites related to primary charge, molar mass, and mass density. *Geochimica et Cosmochimica Acta* 73, 4423–4436.

Jelavić, S., J. Tobler, D., Hassenkam, T., Yoreo, J.J.D., S. Stipp, S.L., K. Sand, K. (2017) Prebiotic RNA polymerisation: energetics of nucleotide adsorption and polymerisation on clay mineral surfaces. *Chemical Communications* 53, 12700–12703.

Kappler, A., Pasquero, C., Konhauser, K.O., Newman, D.K. (2005) Deposition of banded iron formations by anoxygenic phototrophic Fe(II)-oxidizing bacteria. *Geology* 33, 865–868.

Klein, C. (2005) Some Precambrian banded iron-formations (BIFs) from around the world: Their age, geologic setting, mineralogy, metamorphism, geochemistry, and origins. *American Mineralogist* 90, 1473–1499.
Koehler, I., Konhauser, K., Kappler, A. (2010) Role of Microorganisms in Banded Iron Formations. In: *Geomicrobiology: Molecular and Environmental Perspective* (eds. Barton LL, Mandl M, Loy A). Springer Netherlands, Dordrecht, pp. 309–324.
Konhauser, K.O., Planavsky, N.J., Hardisty, D.S., Robbins, L.J., Warchola, T.J., Haugaard, R., Lalonde, S.V., Partin, C.A., Oonk, P.B.H., Tsikos, H., Lyons, T.W., Bekker, A., Johnson, C.M. (2017) Iron formations: A global record of Neoarchaean to Palaeoproterozoic environmental history. *Earth-Science Reviews* 172, 140–177.
Lützenkirchen, J., Preočanin, T., Stipić, F., Heberling, F., Rosenqvist, J., Kallay, N. (2013) Surface potential at the hematite (001) crystal plane in aqueous environments and the effects of prolonged aging in water. *Geochimica et Cosmochimica Acta* 120, 479–486.
Newcomb, C.J., Qafoku, N.P., Grate, J.W., Bailey, V.L., Yoreo, J.J.D. (2017) Developing a molecular picture of soil organic matter–mineral interactions by quantifying organo–mineral binding. *Nature Communications* 8, 396.
Oss, C.J. van (1997) Hydrophobicity and hydrophilicity of biosurfaces. *Current Opinion in Colloid & Interface Science* 2, 503–512.
Phoenix, V.R., Adams, D.G., Konhauser, K.O. (2000) Cyanobacterial viability during hydrothermal biomineralisation. *Chemical Geology* 169, 329–338.
Sand, K.K., Jelavic, S., Dobberschütz, S., Ashby, P.D., Marshall, M.J., Dideriksen, K., Stipp, S.L.S., Kerisit, S.N., Friddle, R.W., DeYoreo, J.J. (2019) Mechanistic Insight into Biopolymer Induced Iron Oxide Mineralization Through Quantification of Molecular Bonding. *ChemRxiv*, https://doi.org/10.26434/chemrxiv.9767504.v1.
Schwertmann, U., Cornell, R.M. (2000) Ferrihydrite. In: *Iron Oxides in the Laboratory*. John Wiley & Sons, Ltd, Weinheim, Federal Republic of Germany, pp. 103–112.
Schwertmann, U., Murad, E. (1983) Effect of pH on the Formation of Goethite and Hematite from Ferrihydrite. *Clays and Clay Minerals* 31, 277–284.
Sun, S., Konhauser, K.O., Kappler, A., Li, Y-L. (2015) Primary hematite in Neoarchean to Paleoproterozoic oceans. *GSA Bulletin* 127, 850–861.
Trainor, T.P., Chaka, A.M., Eng, P.J., Newville, M., Waychunas, G.A., Catalano, J.G., Brown, G.E. (2004) Structure and reactivity of the hydrated hematite (0001) surface. *Surface Science* **573**, 204–224.
Vezenov, D.V., Noy, A., Rozsnyai, L.F., Lieber, C.M. (1997) Force Titrations and Ionization State Sensitive Imaging of Functional Groups in Aqueous Solutions by Chemical Force Microscopy. *Journal of the American Chemical Society* 119, 2006–2015.